10.48047/jocaaa.2024.33.07.40

RADIATIVE NICKEL CHROMIUM IRON ALLOY (NIMONIC 80A) -KEROSENE NANOFLUID FLOW INDUCED BY AN EXPANDING SHEET WITH SLIP FACTOR: A LIE-GROUP ANALYSIS

Arijit Mandal,
Ph. D Scholar in Dr. A. P. J. Abdul Kalam University, Indore, Madhya Pradesh - 452016
Email: arijitmandal.mld@gmail.com

Dr. Annapurna Ramakrishna Sinde,
Department of Mathematics, Dr. A. P. J. Abdul Kalam University, Indore, Madhya Pradesh - 452016
Email: jayabhandari15@gmail.com

Dr. Md Tausif Sk,
Department of Mathematics, Acharya B.N. Seal College, Cooch Behar - 736101, West Bengal, India
E-mail: tausifdropbox@gmail.com

ABSTRACT: In the current review, hydromagnetic convective stream and intensity move of a retaining and electrically leading NIMONIC 80A-kerosene nanofluid over a semi-endless, preferably straightforward, porous extending sheet because of sunlight based radiation is thought of. The stream considered is under both surface and warm slip conditions. The overseeing conditions are changed into a non-direct common differential conditions utilizing traditional Untruth bunch approach which are tackled mathematically through the proficient mathematical shooting procedure with fourth request Runge-Kutta plot. The impacts of involved boundaries on the speed and temperature profiles, skin contact and Nusselt number are inspected and talked about through charts and tables. Correlations with recently distributed works are performed, and fantastic understanding between the outcomes is acquired

Keywords: Nanofluid, Lie group analysis, solar energy radiation, magnetic field, slip conditions.
2010 Mathematics Subject Classification. 76W05

INTRODUCTION:

Sunlight based energy is the most promptly accessible wellspring of energy. It is likewise the most significant of the non-regular wellsprings of energy since it is non-contaminating and, subsequently, helps in decreasing the nursery impact. Sun oriented energy, brilliant light and intensity from the sun, is bridled utilizing a scope of consistently developing innovations like sun powered warming, sun based photovoltaic cells, sunlight based warm power, sun based engineering and fake photosynthesis. Consequently the usage of sunlight based energy and the advances of sun oriented energy materials draw in significantly more consideration in many parts of applied physical science and designing. Nano-materials whose molecule size is more modest than the frequency of de Broglie wave and sound wave are recently evolved energy materials. Subsequently, nanoparticles become to emphatically retain (i.e., skirting middle intensity move steps) and specifically assimilate (i.e., high retention in the sun powered reach and low emittance in the infrared) episode radiation. Chase [12] was the primary who presented the idea of utilizing nanoparticles to gather sun powered energy. Designed suspensions of nanoparticles in fluids, referred to as of late as nanofluid, have produced extensive premium for their true capacities to improve the intensity move rate in designing framework. Nanofluids are produced using materials, like metals (Cu, Ag, Au), oxide ceramics Al2O3, CuO,

10.48047/jocaaa.2024.33.07.40

semiconductors TiO2,SiC, carbon nanotubes and composite materials, for example, alloyed nanoparticles. The base media of nanofluids are typically water, oil, ethylene glycol, CH3)2CO and so forth. Contrasted and traditional intensity move like oil, water and ethylene glycol combination, nanofluids have altogether higher warm conductivity that thus upgrades the intensity move qualities of these liquids.

Regular convection heat move of nanofluid has attracted fascination of numerous analysts late years [1, 2, 4, 7, 11, 15-17, 22, 25, 28, 30, 34, 35]. Normal convection heat move in presence of nanofluids because of sunlight based energy radiation is a significant peculiarity in designing frameworks because of its wide applications in building warming, car innovation, sun oriented innovation, cooling of electronic hardware and so on [5, 10, 23]. Kandasamy et al. [14] concentrated on Hiemenz stream of Cu-nanofluid over a permeable wedge because of sun oriented radiation. As of late, Anbuchezhian et al. [3] have provided details regarding the impacts of cross over attractive field on regular convection stream of a nanofluid because of sun powered energy.

In every one of the previously mentioned papers specialists confined their examinations to stream and intensity move with no-slip limit condition. However, no-slip supposition that isn't valid for liquid streams at the miniature and nano scale. Examination shows that slip stream happens when the trademark size of the stream framework is little or the stream pressure is exceptionally low. To depict the peculiarity of slip, Navier [24] presented a limit condition which expresses that the part of the liquid speed distracting to the limit walls is corresponding to digressive pressure. Afterward, a few specialists [6, 12] expanded the Navier limit conditions. Various examinations have been done scientifically and mathematically with respect to the slip stream systems over surfaces. Martin and Boyd [20] analyzedBlasius limit layer issue within the sight of slip limit condition. These outcomes showed the way that the limit layer condition can be utilized to concentrate on stream at the miniature electro mechanical framework (MEMS) scale and give valuable data to concentrate on the impacts of rarefaction on the shear pressure and design of the stream. In another review [19], they have broke down slip stream and intensity move at steady wall temperature. The hydrodynamic stream within the sight of halfway slip over an extending sheet with pull has been concentrated by Wang [32]. Van Gorder et al. [31] considered the model proposed by Wang [33] depicting the different stream because of an extending surface with both surface slip and pull/infusion. Slip consequences for blended convection stream of a micropolar liquid towards a contracting vertical sheet was concentrated by Das [9]. As of late, Das [8] examined the nanofluid stream over a contracting sheet with surface slip.

Propelled by the above examinations, we plan to explore the impact of slip on the way of behaving of liquid stream and warm vehicle of an engrossing and electrically directing nanofluid over an extending surface because of sun based radiation and within the sight of an outside applied attractive field. The plate is accepted non-reflecting, non-engrossing, in a perfect world straightforward and electrically non-leading in the current work. The paper is coordinated as follows: In segment 2 the numerical examination of the issue is talked about exhaustively. Mathematical analysis is introduced in Segment 3. Segment 4 features the outcomes got through broad calculation. Segment 5 sums up the significant results of the review.

MATHEMATICAL ANALYSIS:

10.48047/jocaaa.2024.33.07.40

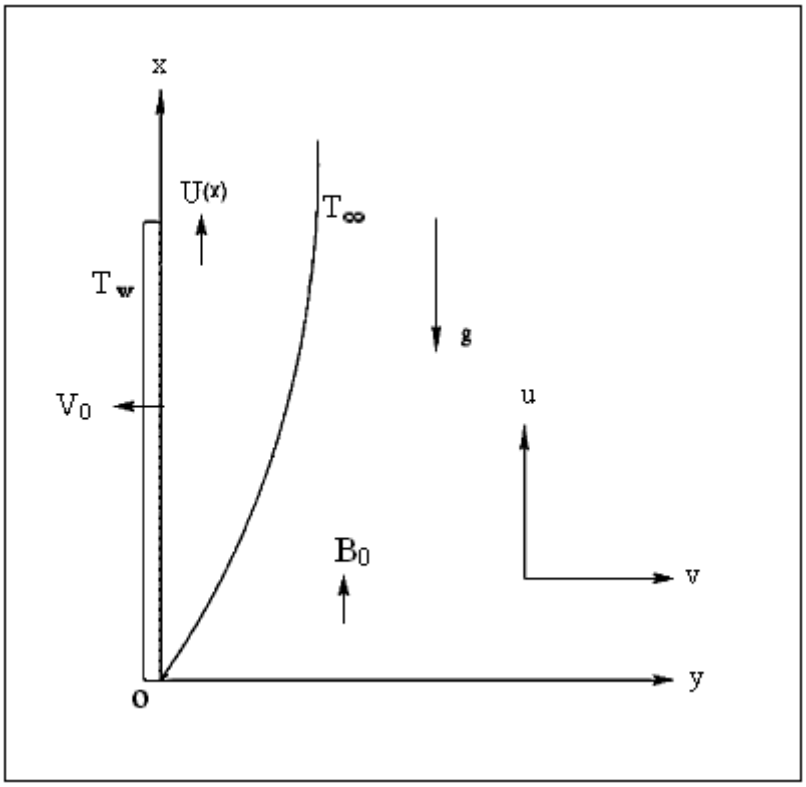

FIGURE 1: PHYSICAL MODEL AND COORDINATE SYSTEM

The consistent two-layered limit layer stream of a thick incompressible electrically directing NIMONIC 80A-kerosene nanofluid over a semi-endless, in a perfect world straightforward, penetrable extending sheet implanted in a liquid immersed permeable medium with surface slip and temperature bounce because of sun oriented radiation is thought of. The direction framework is to such an extent that x estimates the distance along the plate and y estimates the distance regularly into the liquid. The schematics of the issue viable and the direction framework are displayed in Fig.1. An attractive field of uniform strength B_0 is applied in the negative y course consistently. Its collaboration with the electrically leading working nanofluid produces a resistive power, called Lorentz force in the negative x-course. The attractive Reynolds number is thought to be little with the goal that the prompted attractive field is dismissed. What's more, no electric field exists and the Corridor Impact, gooey scattering and Joule warming are completely ignored. The extending surface temperature is considered to have consistent worth T_w, while at a huge worth of y, temperature have steady surrounding esteem T_∞.

It is accepted that the permeable medium is straightforward and in warm balance with the liquid. Likewise, it is accepted that both the liquid and the permeable medium are hazy for self-discharged warm radiation. In the current review, the sun powered radiation is a collimated pillar that is typical to the extending surface. Because of the warming of the retaining nanofluid and the slanted penetrable plate by sunlight based radiation, heat is moved from the plate to the environmental elements. Then again, one might have a non-retaining liquid. For this situation, the strong permeable medium assimilates the episode sun powered radiation and communicates it to the functioning liquid by convection. The thickness of the nanofluid is approximated by the standard Boussinesq model. The consistency and warm conductivity of the nanofluid are considered as factor properties. Under the above presumptions, the limit layer conditions administering the stream and temperature field can be composed as

10.48047/jocaaa.2024.33.07.40

$$\frac{\partial u}{\partial x}+\frac{\partial v}{\partial y}=0 \tag{1}$$

$$u\frac{\partial u}{\partial x}+v\frac{\partial u}{\partial y}=\frac{1}{\rho_{nf}}\left[\mu_{nf}\frac{\partial^2 u}{\partial y^2}+(\rho\beta)_{nf}\,g(\mathrm{T}-\mathrm{T}_\infty)-(\sigma \mathrm{B}_0^2+\frac{\nu_f}{\kappa}\rho_{nf})\,\mathrm{u}\right] \tag{2}$$

$$u\frac{\partial T}{\partial x}+v\frac{\partial T}{\partial y}=\alpha_{nf}\frac{\partial^2 T}{\partial y^2}-\frac{1}{(\rho C)_{nf}}\frac{\partial q''_{rad}}{\partial y}-\frac{Q_0}{(\rho C_p)_{nf}}(\mathrm{T}-\mathrm{T}_\infty) \tag{3}$$

where u, v are the speed parts along the x and y-hub separately, T is temperature, μ_{nf} is the compelling powerful consistency of the nanofluid, B_0 is the uniform attractive field, g is the gravitational speed increase, σ is the electrical conductivity, k is the penetrability of the permeable medium, C_p is the particular intensity at consistent strain, ρ_{nf} is the successful thickness of the nanofluid, α_{nf} is the warm diffusivity of the nanofluid, Q_0 is the temperature subordinate volumetric pace of intensity source/sink and q''_{rad} is the applied retention radiation heat move per unit region. Involving Rosseland estimation for radiation, we can compose

$$q''_{rad}=-\frac{4\sigma_1}{3k^*}\frac{\partial T^4}{\partial y} \tag{4}$$

where σ_1 is the Stefan-Boltzmann constant and k^* is the mean absorption coefficient.

THERMOPHYSICAL PROPERTIES OF NANOFLUID:

In this review, NIMONIC 80A-kerosene nanofluid is utilized as the functioning liquid. The thermophysical properties of the nanofluid associated with the administering conditions are determined utilizing the accompanying conditions (see Maxwell [21], Oztop and Abu-Nothing [26]) and it is recorded in Table 1.

The effective dynamic viscosity of the nanofluid is given by

$$\mu_{nf}=\frac{\mu_f}{(1-\zeta)^{2.5}} \tag{5}$$

where ζ is the solid volume fraction of nanoparticles. The effective density ρ_{nf}, thermal diffusivity α_{nf} and the heat capacitance of the nanofluid $(\rho C_p)_{nf}$ are given by

$$\rho_{nf}=(1-\zeta)\rho_f+\zeta\rho_s \tag{6}$$

$$\alpha_{nf}=\frac{k_{nf}}{(\rho \mathrm{C}_p)_{nf}} \tag{7}$$

$$(\rho \mathrm{C}_p)_{nf}=(1-\zeta)(\rho C_p)_f+\zeta(\rho C_p)_s \tag{8}$$

TABLE 1: THERMOPHYSICAL PROPERTIES OF REGULAR FLUID AND NANOPARTICLES:

Physical Properties	Kerosene	Nimonic 80A
$C_P(\mathrm{J/kg\ K})$	2090	448
$\rho(\mathrm{kg/m^3})$	780	8190
$\kappa(\mathrm{W/mK})$	0.149	112
$\alpha\times10^7(\mathrm{m^2/s})$	1.47	116.3
$\beta\times10^{-5}(1/\mathrm{K})$	99	8.8

10.48047/jocaaa.2024.33.07.40

The thermal conductivity of nanofluid restricted to spherical nanoparticles is approximated by the Maxwell [21]

$$\frac{\kappa_{nf}}{\kappa_f}=\frac{\kappa_s+2\kappa_f-2\zeta(\kappa_f-\kappa_s)}{\kappa_s+2\kappa_f+2\zeta(\kappa_f-\kappa_s)} \tag{9}$$

Here μ_f is the consistency of the base liquid, ρ_f and ρ_s are the densities of the unadulterated liquid and nanoparticles, separately, $(\rho \mathrm{C}_p)_f$ and $(\rho \mathrm{C}_p)_s$ are the particular intensity boundaries of the base liquid and nanoparticles, individually, κ_f and κ_s are the warm conductivities of the base liquid and nanoparticles, individually.

BOUNDARY CONDITIONS:

In the slip flow regime, slip velocity and temperature jump boundary conditions should be applied to the momentum and energy equations. These are

$$u_s=\frac{2-\sigma_v}{\sigma_v}\lambda_0\left(\frac{\partial u}{\partial y}\right)_{y=0} \tag{10}$$

where σ_v is the tangential momentum accommodation coefficient, λ_0 is the molecular mean free path and

$$T_s=\frac{2-\sigma_T}{\sigma_T}\frac{2r}{1+r}\frac{\lambda_0}{\mathrm{Pr}}\left(\frac{\partial T}{\partial y}\right)_{y=0} \tag{11}$$

where σ_T is the thermal accommodation coefficient, Pr is the Prandtl number and r is the specific heat ratio, respectively.

Thus the appropriate boundary conditions for the present problem are

$$\left.\begin{array}{l} u=u_w+u_s,\ \mathrm{v}=\mathrm{V}_0,\ \mathrm{T}=\mathrm{T}_w+T_s \ \text{ at y=0} \\ \mathrm{u}\to 0,\ \mathrm{T}\to T_\infty \ \text{ as } \ \mathrm{y}\to\infty \end{array}\right\} \tag{12}$$

Where u_w=U(=ax) is the velocity of the stretching sheet, a (>0) is the stretching rate (of the sheet) and V_0 is the velocity of suction/injection.

NON-DIMENSIONALIZATION:

Let us introduce the following non-dimensional variables:

$$u'=\frac{u}{\sqrt{a\nu_f}},\ v'=\frac{v}{\sqrt{a\nu_f}},\ x'=\frac{x}{\sqrt{\frac{\nu_f}{a}}},\ y'=\frac{y}{\sqrt{\frac{\nu_f}{a}}},\ \theta=\frac{T-T_\infty}{T_w-T_\infty} \tag{13}$$

Equations (1)-(3) take the non-dimensional form (dropping prime)

$$\frac{\partial u}{\partial x}+\frac{\partial v}{\partial y}=0 \tag{14}$$

$$u\frac{\partial u}{\partial x}+v\frac{\partial u}{\partial y}=\frac{1}{(1-\zeta+\zeta\frac{\rho_s}{\rho_f})}\left[\frac{1}{(1-\zeta)^{2.5}}\frac{\partial^2 u}{\partial y^2}+\left\{1-\zeta+\zeta\frac{(\rho\beta)_s}{(\rho\beta)_f}\right\}\lambda\theta-\left(M^2+K\right)u\right] \tag{15}$$

$$u\frac{\partial \theta}{\partial x}+v\frac{\partial \theta}{\partial y}=\frac{1}{\mathrm{Pr}}\frac{1}{1-\zeta+\zeta\frac{(\rho \mathrm{C}_p)_s}{(\rho \mathrm{C}_p)_f}}\left[\frac{\kappa_{nf}}{\kappa_f}\frac{\partial^2\theta}{\partial y^2}+\frac{4}{3}N\left\{\frac{\partial}{\partial y}\left(C_T+\theta\right)^3\right\}\frac{\partial\theta}{\partial y}-\theta\delta\right] \tag{16}$$

with the boundary conditions

10.48047/jocaaa.2024.33.07.40

$$\left.\begin{array}{l} u = x + \gamma \dfrac{\partial u}{\partial y},\ v = \dfrac{V_0}{\sqrt{a\nu_f}},\ \theta = 1 + \xi \dfrac{\partial \theta}{\partial y} \ \text{ at } \ y = 0 \\ u \to 0,\ \theta \to 0 \ \ as \ \ y \to \infty \end{array}\right\} \tag{17}$$

where M= $B_0\sqrt{\dfrac{\sigma}{a\rho_f}}$ is the magnetic field parameter, $\lambda = \dfrac{g(\rho\beta)_f (T_w - T_\infty)}{a\rho_f U}$ is the natural convection parameter, K= $\dfrac{\nu_f}{k}$ is the permeability parameter of the porous media, Pr= $\dfrac{\nu_f}{\alpha_{nf}}$ is the Prandtl number, N = $\dfrac{4\sigma_1 T_\infty^3}{(\rho C_p)_f k^*}$ is the radiation parameter, $C_T = \dfrac{T_\infty}{T_w - T_\infty}$ is the temperature ratio where C_T assumes very small values by its definition as $T_w - T_\infty$ is very large compared to T_∞, $\delta = \dfrac{Q_0 \nu^2{}_f (T_w - T_\infty)}{\kappa_f U^2}$ is the heat source/sink parameter, $\gamma = \dfrac{2-\sigma_v}{\sigma_v}\sqrt{\dfrac{a}{\nu_f}\lambda_0}$ is the slip velocity parameter and $\xi = \dfrac{2-\sigma_T}{\sigma_T}\dfrac{2r}{1+r}\dfrac{\lambda_0}{\Pr}\sqrt{\dfrac{a}{\nu_f}}$ is the thermal slip parameter.

The introduction of the stream function $\psi(x, y)$, defined by u= $\dfrac{\partial \psi}{\partial y}$ and v = - $\dfrac{\partial \psi}{\partial x}$, leads to Eqs. (15),(16) taking the following form:

$$\frac{\partial \psi}{\partial y}\frac{\partial^2 \psi}{\partial x \partial y} - \frac{\partial \psi}{\partial x}\frac{\partial^2 \psi}{\partial y^2} = \frac{1}{(1-\zeta+\zeta\frac{\rho_s}{\rho_f})}\left[\frac{1}{(1-\zeta)^{2.5}}\frac{\partial^3 \psi}{\partial y^3} + \left\{1-\zeta+\zeta\frac{(\rho\beta)_s}{(\rho\beta)_f}\right\}\lambda\theta - \left(M^2+K\right)\frac{\partial \psi}{\partial y}\right]$$

(18)

$$\frac{\partial \psi}{\partial y}\frac{\partial \theta}{\partial x} - \frac{\partial \psi}{\partial x}\frac{\partial \theta}{\partial y} = \frac{1}{\Pr}\frac{1}{1-\zeta+\zeta\frac{(\rho C_p)_s}{(\rho C_p)_f}}\left[\frac{\kappa_{nf}}{\kappa_f}\frac{\partial^2 \theta}{\partial y^2} + \frac{4}{3}N\left\{\frac{\partial}{\partial y}\left(C_T+\theta\right)^3\right\}\frac{\partial \theta}{\partial y} - \theta\delta\right] \tag{19}$$

with the boundary conditions

$$\left.\begin{array}{l} \dfrac{\partial \psi}{\partial y} = x + \gamma \dfrac{\partial^2 \psi}{\partial y^2},\ \dfrac{\partial \psi}{\partial x} = -\dfrac{V_0}{\sqrt{a\nu_f}},\ \theta = 1 + \xi \dfrac{\partial \theta}{\partial y} \ \text{ at } \ y = 0 \\ u \to 0,\ \theta \to 0 \ \ as \ \ y \to \infty \end{array}\right\} \tag{20}$$

SYMMETRY GROUPS OF EQUATIONS:

The evenness gatherings of conditions (18),(19) are determined utilizing traditional Falsehood bunch approach. The one-boundary minuscule Falsehood gathering of changes leaving (18), (19) invariant is characterized as

$$\left.\begin{array}{l} x^* = x + \varepsilon\xi_1(x, y, \psi, \theta),\ y^* = y + \varepsilon\xi_2(x, y, \psi, \theta), \\ \psi^* = \psi + \varepsilon\eta_1(x, y, \psi, \theta),\ \theta^* = \theta + \varepsilon\eta_2(x, y, \psi, \theta) \end{array}\right\} \tag{21}$$

where is the boundary of the gathering. Eq. (21) might be considered as a point-change which changes directions (x, y, ψ, θ) to the directions $\left(x^*, y^*, \psi^*, \theta^*\right)$.

Via doing a straight forward however drawn-out polynomial math, the type of the infinitesimals can be gotten as

10.48047/jocaaa.2024.33.07.40

$$\xi_1 = d_1 x + d_2,\ \xi_2 = g(\mathrm{x}),\ \eta_1 = d_3\psi + d_4,\ \eta_2 = d_5 \tag{22}$$

where d_1, d_2, d_3, d_4 and d_5 are erratic boundaries and the boundary addresses the scaling change and g(x) is an inconsistent capability.

Forcing the limitations from the limit conditions on the infinitesimals, one might get the accompanying structure for Eq. (22)

$$\xi_1 = d_1 x,\ \xi_2 = 0,\ \eta_1 = d_3\psi,\ \eta_2 = 0 \tag{23}$$

The relations (23) lead to the following characteristic equations for similarity:

$$\frac{dx}{x} = \frac{dy}{0} = \frac{d\psi}{\psi} = \frac{d\theta}{0} \tag{24}$$

from which the similarity variables, velocity and temperature turn out to be of the form

$$\eta = y,\ \psi = xf(\eta) \text{ and } \theta = \theta(\eta) \tag{25}$$

Substituting equation (25) into equations (18), (19), one may finally obtain the system of nonlinear ordinary differential equations

$$f'''+(1-\zeta)^{2.5}\left[\left(1-\zeta+\zeta\frac{\rho_s}{\rho_f}\right)\left(ff''-f'^2\right)-\left(M^2+K\right)f'+\left\{1-\zeta+\zeta\frac{(\rho\beta)_s}{(\rho\beta)_f}\right\}\lambda\theta\right]=0 \tag{26}$$

$$\frac{k_{nf}}{k_f}\theta''-\delta\theta+\frac{4}{3}N\left\{\left(C_T+\theta\right)'\right\}'+\Pr\left(f\theta'-f'\theta\right)\left\{1-\zeta+\zeta\frac{(\rho c_p)_s}{(\rho c_p)_f}\right\}=0 \tag{27}$$

where prime denotes differentiation with respect to η

The corresponding boundary conditions become

$$\left.\begin{aligned} &f = S,\ f' = 1+\gamma f'',\ \theta = 1+\xi\theta' \text{ at } \eta=0\\ &f' \to 0,\ \theta \to 0 \text{ as } \eta \to \infty \end{aligned}\right\} \tag{28}$$

where S=- $\frac{V_0}{\sqrt{a\nu_f}}$, S>0corresponds to suction and S<0 corresponds to injection.

PHYSICAL QUANTITIES OF INTEREST:

The quantities of physical interest in this problem are the skin friction coefficient and the local Nusselt number which are defined as follows:

$$C_f = \frac{\mu_{nf}}{\rho_f U^2}\left(\frac{\partial u}{\partial y}\right)_{y=0} = -\frac{1}{(1-\zeta)^{2.5}}(\mathrm{Re}_x)^{-\frac{1}{2}} f''(0) \tag{29}$$

$$\mathrm{Nu} = \frac{xk_{nf}}{k_f(\mathrm{T}_w-\mathrm{T}_\infty)}\left(\frac{\partial T}{\partial y}\right)_{y=0} - \frac{4\sigma_1}{3k^*}\left(\frac{\partial T^4}{\partial y}\right)_{y=0} = -\left(\mathrm{Re}_x\right)^{\frac{1}{2}}\frac{k_{nf}}{k_f}\theta'(0)\left[1+\frac{4}{3}N\left\{C_T+\theta(0)\right\}^3\right] \tag{30}$$

where $\mathrm{Re}_x = \frac{U_x}{\nu_f}$ is the local Reynolds number. Thus the reduced skin friction coefficient $C_f r$ and the reduced Nusselt number Nur can be as

$$C_f r = \mathrm{Re}_x^{\frac{1}{2}} C_f = -\frac{1}{(1-\zeta)^{2.5}} f''(0) \tag{31}$$

$$\mathrm{Nur} = \mathrm{Re}_x^{-\frac{1}{2}} Nu = -\frac{k_{nf}}{k_f}\theta'(0)\left[1+\frac{4}{3}\left\{C_T+\theta(0)\right\}^3\right] \tag{32}$$

TABLE 2: COMPARISONS OF RESULTS FOR -$\theta'(0)$ WITH PREVIOUSLY PUBLISHED WORK:

10.48047/jocaaa.2024.33.07.40

Pr	Wang [33]	Anbuchezhian et al. [3]	Present Study
0.07	0.0656	0.0655580	0.0655578
0.20	0.1691	0.1690967	0.1690953
0.70	0.4539	0.4539134	0.4539130
2.00	0.9114	0.9113678	0.9113666
7.00	1.8954	1.8953998	1.8953999
20.0	3.3539	3.3538999	3.3538999
70.0	6.4622	6.46219997	6.4621968

NUMERICAL EXPERIMENT:

METHOD OF SOLUTION:

The arrangement of conditions (26), (27) being exceptionally non-straight can't be addressed logically. These coupled conditions have been settled mathematically by applying the Nachtsheim and Swigert (see Kafoussias and Williams [14]) shooting cycle method along with Runge-Kutta fourth-request reconciliation conspire. The unknown beginning circumstances are expected and afterward incorporated mathematically as an underlying worth issue to a given terminal point. Improvement is made on the upsides of accepted missing beginning circumstances by iteratively contrasting the determined worth of the reliant variable at the terminal point with its given worth there. A stage size of $\Delta\eta$=0.01 has been chosen to be palatable for a combination rule of 10^{-6} in all cases.

TABLE 3: EFFECTS OF VARIOUS PARAMETERS ON $C_f r$ AND Nur:

ζ	γ	ξ	M	N	$C_f r$	Nur
0	0.2	0.3	0.5	0.2	1.38397	4.0471
0.05					1.61773	4.29743
0.1					1.8739	4.55141
0.15					2.15855	4.81379
0.05	0				2.35023	4.67176
	0.2				1.61773	4.29743
	0.4				1.24842	4.05833
	0.6				1.02152	3.88535
	0.1	0			1.91814	4.96337
		0.03			--	4.45961
		0.06			--	4.02269
		0.1			--	3.53826
		0.03	0.5		1.91814	4.45961
			1		2.01153	4.4232
			2		2.18974	4.3591
			5		2.60095	4.21082
			0.5	0	1.9057	4.15859
				0.2	--	4.45961
				0.4	--	4.71725
				0.6	--	4.94103

CODE VERIFICATION:

10.48047/jocaaa.2024.33.07.40

As a trial of the exactness of the arrangement, the upsides of $\theta'(0)$ are contrasted and Anbuchezhian et al. [3] and Wang [33] for different upsides of Pr without any outside heat source/sink, nanoparticles, slip speed, warm slip, sun oriented radiation and magneticfield in table 2. Table shows that the mathematical outcomes acquired by the current code and the outcomes announced by Anbuchezhian et al. [3] and Wang [33] are in generally excellent understanding. In this manner the utilization of the present mathematical code for current model is legitimate.

RESULTS AND DISCUSSIONS:

In this part, we present our discoveries in even and graphical structures to explore the significant highlights of the answer for a scope of upsides of the boundaries influencing the stream and intensity move peculiarities. The mathematical outcomes for dimensionless speed $f'(\eta)$ and temperature $\theta(\eta)$ are figured for the accompanying general qualities: M=0.5, K=1.0, λ =-1.2, =0.1, ξ =0.05, N=0.2, S=1.2 and ζ =0.05 except if generally indicated.

Table 3 present the impacts for different upsides of the radiation boundary N, slip speed boundary , warm slip boundary , nanoparticle volume part and attractive field boundary M on the decreased skin grating coefficient and the diminished Nusselt number Nur. From Table, it could be seen that the diminished skin rubbing coefficient at the wall diminishes with an expansion in the slip boundary. This is less articulated with an expansion in the worth of . That is, true to form, for the liquid streams at nano scales, the shear pressure at the wall diminishes with an expansion in the slip boundary. One may noticed that in the no slip condition issue the most elevated wall shear pressure happens. Additionally, the Nusselt number reductions with the expansion in slip boundary for NIMONIC 80A-kerosene nanofluid. Further, it is seen from table that an expansion in warm slip boundary prompts decline in the upsides of the pace of intensity move at the limit mass of the plate. In this manner, it is attractive, to arrive at a high intensity move rate, less slip on the wall by a fluid with a high Prandtl number is required. It tends to be seen that the intensity move rate at the plate increments with expanding upsides of radiation boundary impact isn't noticeable on . It is essential that the sunlight based radiation impact applies serious areas of strength for an on the intensity move at the plate; upgrading it by close to around 27% as the radiation boundary changes from 0.0 to 1.0. This improvement is expected to the nanoparticles of high warm conductivity being driven away from the hot sheet to the peaceful nanofluid. The wall skin grating coefficient increments with an expansion in the nanoparticle volume part as displayed in Table 3. It is likewise found from this table that the presence of nanoparticles brings about an increment of the decreased Nusselt number.

Presently, the graphical outcomes that give extra knowledge into the issue being scrutinized are examined as follows:

10.48047/jocaaa.2024.33.07.40

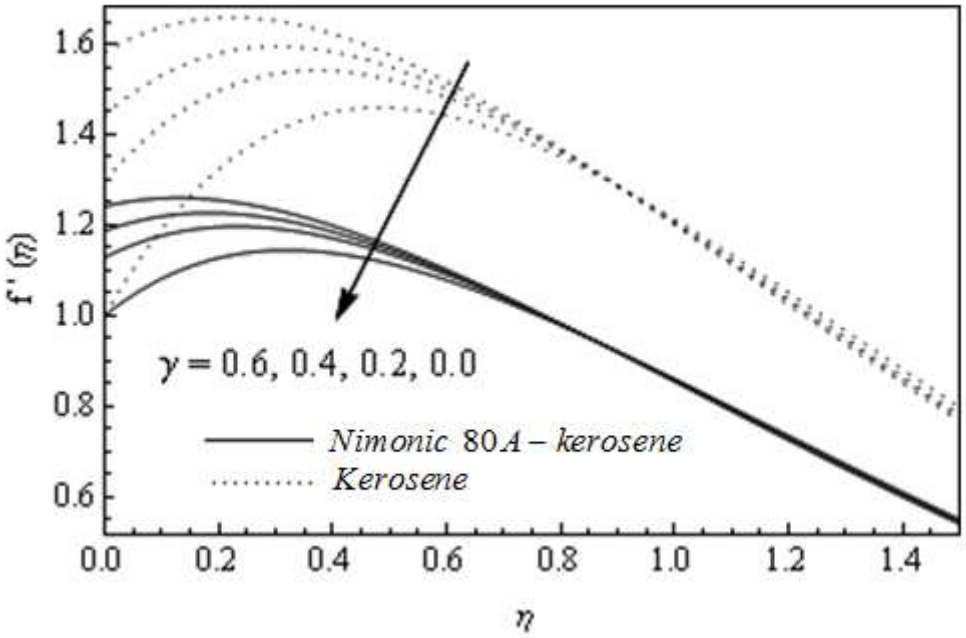

FIGURE 2: VELOCITY PROFILES FOR VARIOUS VALUES OF γ

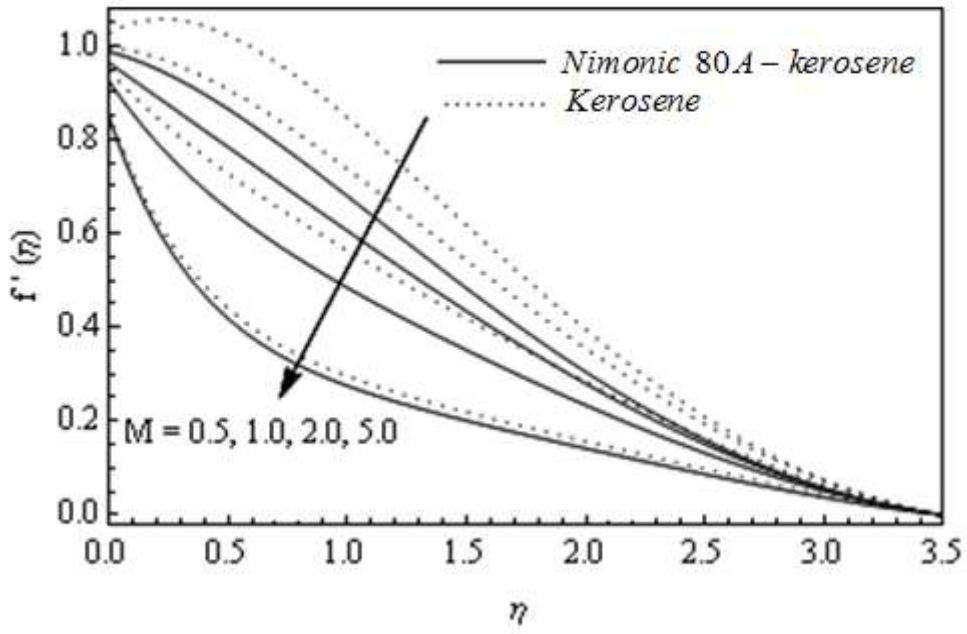

FIGURE 3: VELOCITY PROFILES FOR VARIOUS VALUES OF M

10.48047/jocaaa.2024.33.07.40

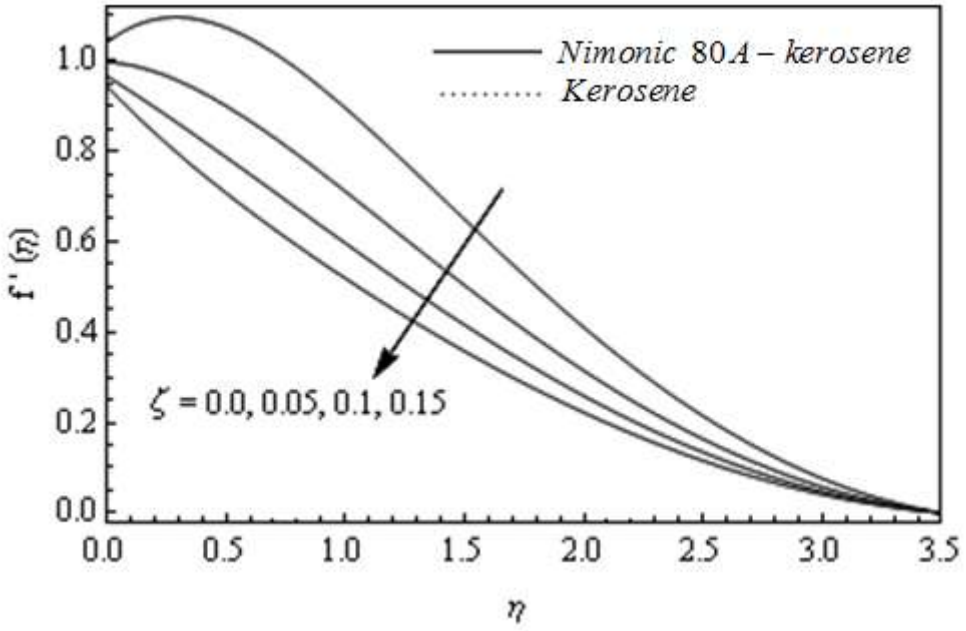

FIGURE 4: VELOCITY PROFILES FOR VARIOUS VALUES OF ζ

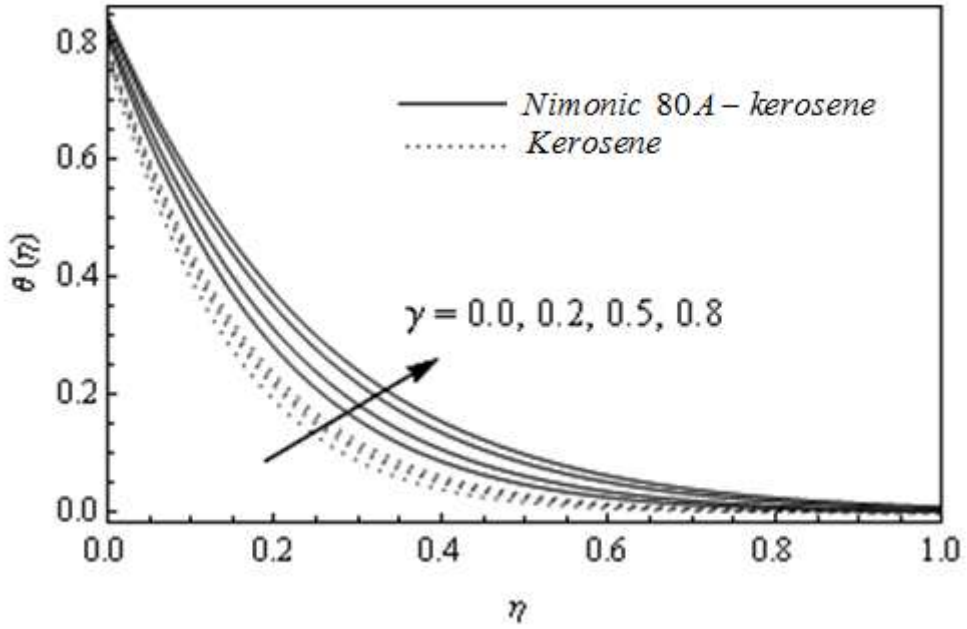

FIGURE 5: TEMPERATURE PROFILES FOR VARIOUS VALUES OF γ

COMPUTATIONAL RESULTS FOR VELOCITY PROFILES:

Fig.2 draws out the impact of slip boundary on the liquid speed. As slip boundary expands, the slip at the surface mass of the plate increments. In this way the liquid speed increments with the increment of slip boundary in presence of sun powered radiation for $\eta < 0.7$ (not set in stone). Be that as it may, the impact isn't critical for $\eta > 0$. (still up in the air). This yields an expansion in the limit layer thickness. Consequently hydrodynamic limit layer thickness increments as the slip boundary increments for both the customary (kerosene)and nanofluid and accordingly, the neighborhood speed additionally increments. The physical science behind

10.48047/jocaaa.2024.33.07.40

this is that the expanded slip boundary close to the wall district diminishes the speed slope at there. In the no-slip condition, approaches zero, so the slip speed at the wall is equivalent to nothing (i.e., u_s =0), in like manner the liquid velocity adjacent to the wall is equivalent to the speed of the extending surface (u_w), then, at that point, f'(0)=1. It ought to be noticed that the impact of slip boundary is unmistakable for kerosene than NIMONIC 80A-kerosene nanofluid. The impact of attractive field boundary M on the liquid speed is portrayed in Fig.3. It is seen from the figure that the liquid speed diminishes with an expansion in the upsides of M close to the limit layer district thus diminishes the thickness of force limit layer. The purpose for this peculiarity is that use of attractive field to an electrically leading nanofluid brings about a resistive sort force called the Lorentz force. This power tends to dial back the movement of the nanofluid in the limit layer district. Figs. 4 delineate the variety of the speed circulation for different upsides of the nanoparticle volume division boundary . It is seen from the figure that the speed conveyance across the limit layer diminishes with the increment of ζ for NIMONIC 80A-kerosene. Subsequently the force limit layer thickness diminishes and tends asymptotically to zero as the distance increments from the limit. This responsiveness of the limit layer thickness to the volume part of nanoparticles is connected with the expanded warm conductivity of the nanofluid. Truth be told, higher upsides of the warm conductivity are joined by higher upsides of warm diffusivity.

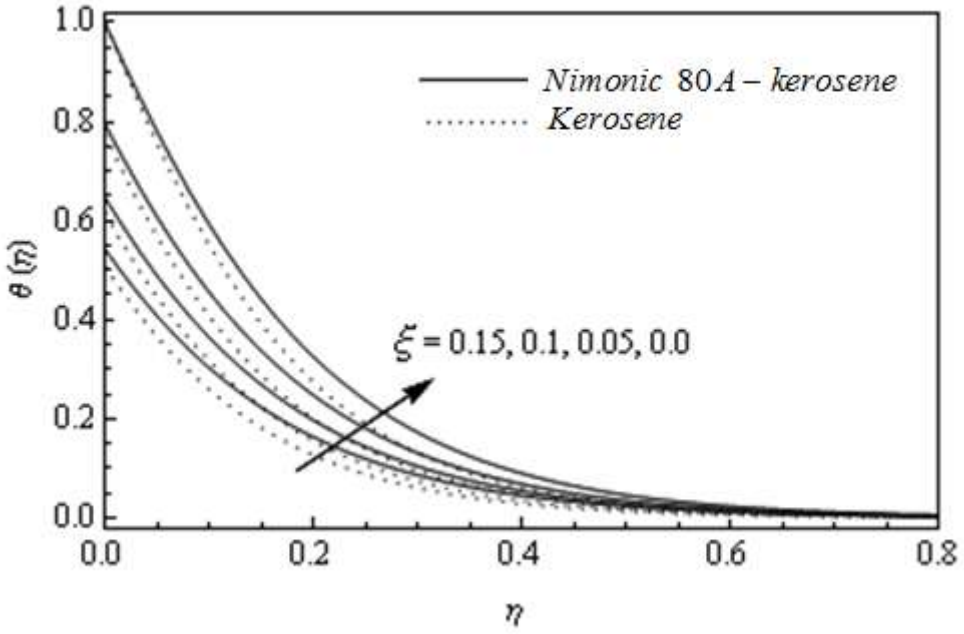

FIGURE 6: TEMPERATURE PROFILES FOR VARIOUS VALUES OF ξ

10.48047/jocaaa.2024.33.07.40

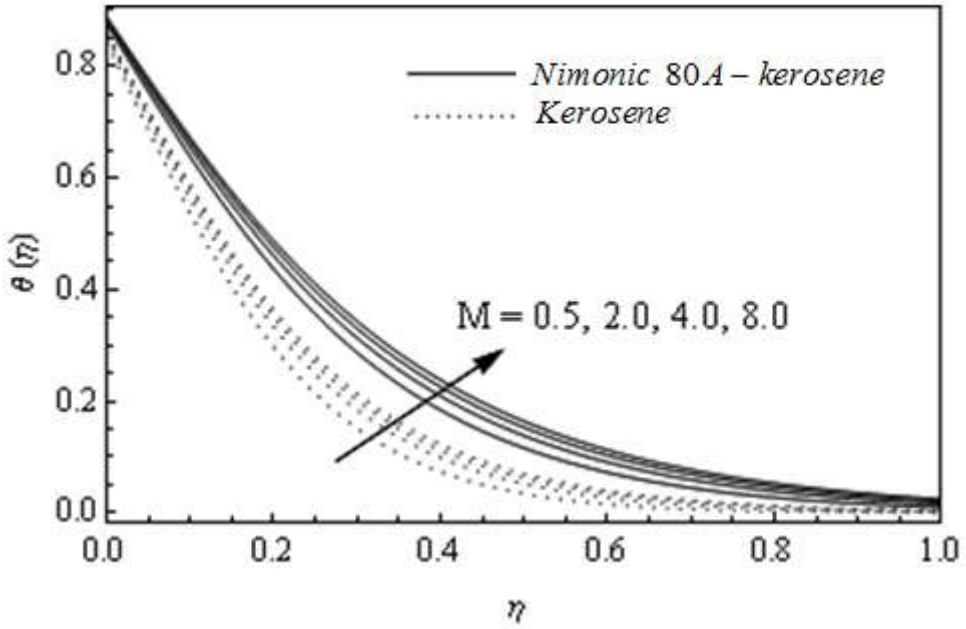

FIGURE 7: TEMPERATURE PROFILES FOR VARIOUS VALUES OF M

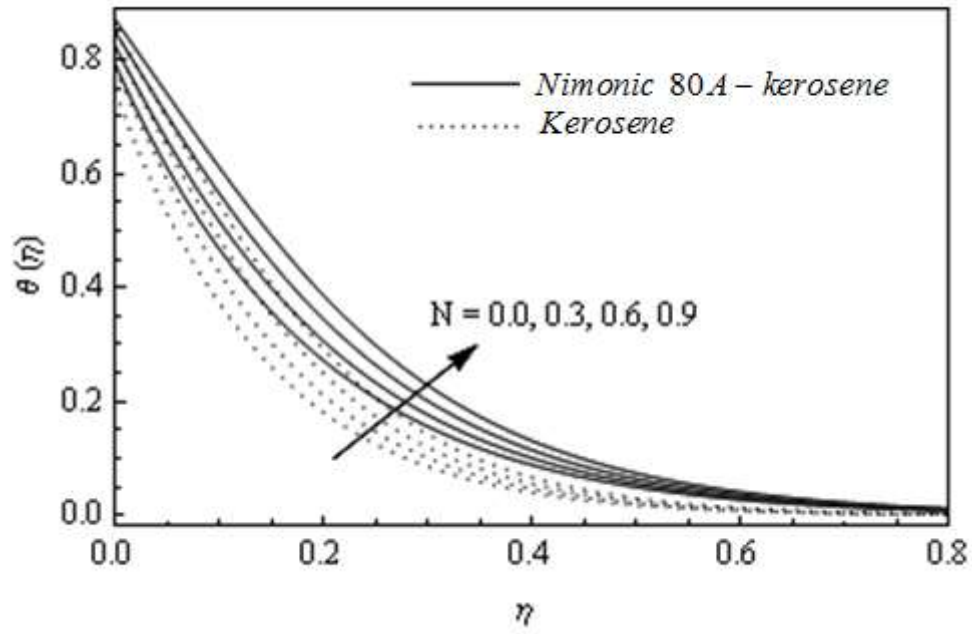

FIGURE 8: TEMPERATURE PROFILES FOR VARIOUS VALUES OF N

10.48047/jocaaa.2024.33.07.40

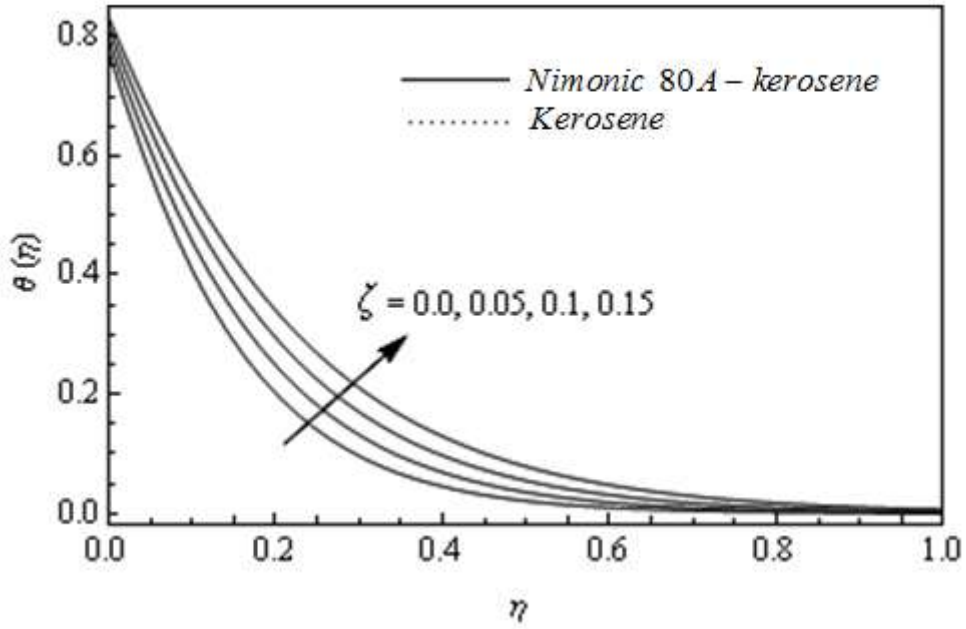

FIGURE 9: TEMPERATURE PROFILES FOR VARIOUS VALUES OF ζ

COMPUTATIONAL RESULTS FOR TEMPERATURE PROFILES:

The impact of slip speed boundary on temperature dissemination is displayed in Fig.5. Figure demonstrates that an increment of slip boundary will in general build the temperature into the liquid field for both NIMONIC 80A-kerosene nanofluid and standard liquid i.e., kerosene however impact isn't critical for customary liquid i.e., for kerosene in contrast with the nanofluid. Subsequently, by heightening, warm limit layer thickness upgrades. In this way, we can decipher that the pace of intensity move diminishes with the expansion in slip boundary. This peculiarity is more unmistakable within the sight of nanoparticles. Fig.6 presents the impact of warm slip boundary on liquid temperature within the sight of sun based radiation. It is seen from the figure that without any warm slip boundary for example when =0, the temperature of the liquid and that of the extending surfaces is same, which in the current issue is one i.e., =1. As the slip boundary expands, the temperature of the liquid abatements close to the limit layer locale and consequently the thickness of warm limit layer diminishes. It is worth for referencing that these profiles fulfill the far field limit conditions asymptotically, which support the mathematical outcomes got. The impact of attractive field on the liquid temperature is delineated in Fig. 7. Figure shows that the liquid temperature is the most extreme close to the limit layer area and it diminishes on expanding the limit layer direction to move toward free stream esteem. Likewise liquid temperature increments with expanding the upsides of M in the limit layer locale and, as a result, thickness of the warm limit layer increments. The effect of radiation boundary N on the temperature profiles is introduced in fig. 8. It can without much of a stretch be seen from figure that the temperature diminishes as the limit layer coordinate increments for a proper worth of N however the pace of decline is quicker as worth of N continues expanding. For a non-zero fixed worth of , temperature dispersion across the limit layer increments with the rising upsides of N and consequently the thickness of warm limit layer increments. Another significant truth is that the impact of N is more huge for NIMONIC 80A-kerosene nanofluid than that of standard liquid. Fig. 9 exhibits the impact of nanoparticle volume part boundary on nanofluid temperature within the sight of intensity source/sink. It is seen from the figure that temperature upgrades on expanding in the limit layer area and is most extreme at the outer layer of the plate. Accordingly, the presence of nanoparticles, specifically

10.48047/jocaaa.2024.33.07.40

NIMONIC 80A prompts an expansion in the thickness of the warm limit layer profile and tends asymptotically to zero as the distance increments from the limit.

CONCLUSIONS:

In the current review, the impact of slip speed and warm slip on the way of behaving of liquid stream and warm vehicle of an engrossing and electrically leading nanofluid over an extending surface because of sun powered radiation and within the sight of an outer applied attractive field is examined utilizing mathematical procedure. Lie bunch changes are applied to the overseeing conditions. The diminished non-straight normal differential conditions are tackled mathematically by utilizing Runge-Kutta-Fehlberg strategy with shooting procedure. The accompanying end can be drawn from the current examination:

- In limit layer district, the speed of the liquid increments with the increment of slip boundary
- be that as it may, impact is converse for attractive field boundary M and nanoparticle volume portion
- An expansion in the slip speed, sun oriented radiation and nanoparticles volume part lead to build the warm boundary layer thickness yet inverse impact happens for warm slip.
- The skin contact coefficient increments with the expansion in the nanoparticle volume portion and attractive field boundary M while it diminishes with slip boundary.
- The rising upsides γ , M and ξ are to diminish the decreased Nusselt number; thus, less intensity is conveyed out of the sheet, bringing about an increment of the warm limit layer thickness and subsequently diminishing the intensity move rate but the nature is inverse for sun powered radiation boundary N and nanoparticle volume division .
- The outcomes show that nanofluid plainly decrease heat move rate contrasted with their own base liquid.
- The restricting instance of the current outcomes ($\gamma = \xi = 0$) is in superb concurrence with the aftereffects of Anbuchezhian et al. [3].

REFERANCES:

[1] Abu-Nada E, Masoud Z, Hijazi A.: Natural convective heat transfer enhancement in horizontal concentric annuli using nanofluids. Int Commun Heat Mass Transf 35(5):657-665 (2008).

[2] Aminossadati SM, Ghasemi B,: Natural convection of water- CuO nanofluid in a cavity with two pairs of heat source-sink. Int Commun Heat Mass Transf 38:672-678 (2011)

[3] Anbuchezhian N, Srinivasan K, Chandrasekaran K, Kandasamy R,: Magnetohydrodynamic effects on natural convection flow of a nanofluid in the presence of heat source due to solar energy. Meccanica 48: 307-321 (2013)

[4] Aziz A, Khan WA,: Natural convective boundary layer flow of a nanofluid past a convectivly heated vertical plate. Int J Therm Sci 52:83-90 (2012)

[5] Chamkha AJ, Issa C, Khanafer K,: Natural convection from an inclined plate embedded in a variable porosity porous medium due to solar radiation. Int J Therm Sci 41:73-81(2002)

[6] Choi CH, Westin JA, Breuer KS,: To slip or not to slip water flows in hydrophilic and hydrophobic microchannels. in; Proceedings of IMECE New Orlaneas LA Paper No 2002-33707(2002)

[7] Clausing A,: Analysis of convective losses from cavity solar central receivers. Solar Energy 27:295-300 (1981)

[8] Das K,: Nanofluid flow over a shrinking sheet with surface slip. Microfluidics and Nanofluidics (On line published) DOI 10.1007/s10404-013-1216-7 (2013)

10.48047/jocaaa.2024.33.07.40

[9] Das K,: Slip effects on MHD mixed convection stagnation point flow of a micropolar fluid towards a shrinking vertical sheet. Comput Math Appls 63:255-267 (2012)
[10] Dehghan AA, Behnia M,: Combined natural covection conduction and radiation heat transfer in a discretely heated open cavity. ASME J Heat Transf 118:54-56 (1996).
[11] Hamad MAA, Ferdows M: Similarity solution of boundary layer stagnation point flow towards a heated porous stretching sheet saturated with a nanofluid with heat absorption/generation and suction/blowing: A lie group analysis. Commun nonlinear Sci Numer Simulat. 17:132-140 (2012).
[12] Hina S, Hayat T, Alsaedi A: Slip Effects on MHD Peristaltic Motion with Heat and Mass Transfer. Arab. Jour. Sci. Engg. 39(2), 593-603 (2014)
[13] Hunt AJ,: Small particle heat exchangers.Report LBL-78421 for the US Department of Energy, Lawrence Berkeley Laboratory (1978)
[14] Kafoussias NG, Williams NG,: Thermal-diffusion and diffusion-thermo effects on mixed free-forced convective and mass transfer boundary layer flow with temperature dependent viscosity. Int J Engg Sci 33:1369–1384 (1995)
[15] Kandasamy R, Muhaimin I, Khamis AB, Roslan RB,: Unsteady Hiemenz of Cu-nanofluid over a porous wedge in the presence of thermal stratification due to solar energy radiation: Lie group transformation. Int J Therm Sci 65:196-205 (2013)
[16] Khan WA, Aziz A,: Natural convection flow of a nanofluid over a vertical plate with uniform surface heat flux. Int J Therm Sci 50:1207-1214(2011)
[17] Khanafer K, Vafai K, Lightstone M,: Buoyancy driven heat transfer enhancement in a two-dimensional enclosure utilizing nanofluids. Internatioal J Heat Mass Transf 46:3639-3653(2006)
[18] Kuznetsov AV, Nield DA, Natural convective boundary layer flow of a nanofluid past a vertical plate. Int J Therm Sci 49:243-247(2010)
[19] Martin MJ, Boyd ID,: Momentum and heat transfer in a laminar boundary layer with slip flow. J Thermophy Heat Transf 20(4):710-719 (2006)
[20] Martin MJ, Boyd ID,: Blasius boundary layer solution with slip flow conditions. Presented at the 22nd Rarefied Gas Dynamics Symposium Sydney Australia (2000)
[21] Maxwell J (1904) A treatise on electricity and magnetism. second ed Oxford University Press Cambridge UK.
[22] Moradi A, Alsaedi A, Hayat T: Investigation of Nanoparticles Effect on the Jeffery–Hamel Flow. Arab. Jour. Sci. Engg. 38(10), 2845-2853 (2013)
[23] Muftuoglu A, Bilgen E,: Heat transfer in inclined rectangular receivers for concentrated solar radiation. Int Commun Heat Mass Transf 35:551-556(2008)
[24] Navier CLMH,: Mémoire sur les lois du mouvement des fluids. Mém Acad Roy Sci Inst France 6:389-440 (1823)
[25] Noghrehabadi A, Samimi A,: Natural convective heat transfer of nanofluids due to thermophoresis and Brownian diffusion in a square enclosure. Int J Engg Adv Tech 1:88-93(2012)
[26] Oztop HF, Abu-Nada E,: Numerical study of natural convection in partially heated rectangular enclosers with nano-fluids. Int J Heat Fluid Flow 29:1326-1336 (2008)
[27] Richard KS, Lee SM,: 800 hours of operational experience from a 2 kW solar dynamic system. In: El-Genk MS(ed.)Space technology and application international forum 426-1431(1999)
[28] Saedodin S, Shahbabaei M. Thermal Analysis of Natural Convection in Porous Fins with Homotopy Perturbation Method (HPM). Arab. Jour. Sci. Engg. 38(8), 2227-2231 (2013)
[29] Trieb F, Nitsch J,: Recommendations for the market introduction of solar thermal power stations. Renew Energy 14:17-22 (1998)

10.48047/jocaaa.2024.33.07.40

[30] Vajravelu K, Prasad KV, Lee J, Lee C, Pop I, Van Gorder RA,: Convective heat transfer in the flow of viscous Ag-Water and Cu-Water nanofluids over a stretching surface. Int J Therm Sci 50:843-851 (2011)
[31] Van Gorder RA, Sweet E, Vajravelu K,: Nano boundary layers over stretching surfaces. Commun Nonlinear Sci Num Simul 15:1494-1500 (2010)
[32] Wang CY,: Analysis of viscous flow due to a stretching sheet with surface slip and suction. Nonlinear Analy Real World Appls 10(1):375-380(2009)
[33] Wang CY,: Free convection on a vertical stretching surface. J Appl Maths Mechs 69:418-420(1989)
[34] Yazdi M, Moradi A, Dinarvand S : MHD Mixed Convection Stagnation-Point Flow Over a Stretching Vertical Plate in Porous Medium Filled with a Nanofluid in the Presence of Thermal Radiation Arab. Jour. Sci. Engg. 39(3), 2251-2261 (2014)
[35] Zafariyan S, Fanaee A, A. Mohammadzadeh A: The Investigation of Thermal and Solutal Secondary Effects on MHD Convective Transfer Past a Vertical Surface in a Porous Medium Arab. Jour. Sci. Engg. 38(11), 3211-3220 (2013)